DETECTION OF DUST PARTICLES BY LASER HEATING

E. Stoffels, W.W. Stoffels, G.M.W. Kroesen and F.J. de Hoog,
Department of Physics, Eindhoven University of Technology,
P.O. Box 513, 5600 MB Eindhoven, The Netherlands.

Abstract

Laser heating of particles formed in an Ar/CCl_2F_2 rf plasma has been studied. Time resolved spectra show blackbody-like curves with temperatures between 2600 K and 3600 K. The time delay between the onset of the laser pulse and the particle emission is due to heating of the clusters. It depends on the particle radius and the laser fluence. A model for heating and thermal decomposition of the clusters has been developed. This model gives a very good description of the observed phenomena. Laser heating allows to determine the particle size and density from a single measurement.

Introduction

Particle formation in surface processing plasmas is a widely recognized problem [1, 2]. As present research aims at a full control of particle containing plasmas, one of the major experimental tasks is the *in situ* determination of the particle size and density. The commonly used laser light scattering is an experimentally easy technique, but the interpretation of the data is tedious and requires knowledge (or assumptions) of the refractive index of the material. For particles much smaller than the wavelength of the scattered light (i.e. in the Rayleigh scattering regime) the efficiency of scattering decreases drastically as the intensity is proportional to the sixth power of the radius. We propose a new detection method based on laser heating of the dust particles. A high power laser is used to heat the particles and the subsequent bright white light emission is monitored by means of time resolved optical emission spectroscopy. The broad band emission intensity is much stronger than the laser scattering signal and the intensity ratio increases for smaller particles [3]. Moreover, this technique is free from stray light problems, which disturb scattering experiments.

Theory

When a laser beam strikes the cluster surface, part of the energy is absorbed, causing the particle to be heated. Energy is lost by radiation, thermal conduction

and evaporation or decomposition of the particle [4]. At low pressures thermal conduction can be neglected and radiation losses become important only at very high temperatures (above 5000 K), which are not realistic in our case. Therefore the absorbed laser energy is consumed by heating and evaporation of the particles. The energy losses due to particle evaporation or thermal decomposition can be related to the decrease rate of the particle radius: $H/V_m(dr/dt)$, where H (about 3 eV) is the energy of the decomposition process (J/released molecule) and V_m the molecular volume in the solid state of the released species (m^3/molecule). The energy balance for a particle can be now written as:

$$\frac{4}{3}r\rho C\frac{dT}{dt} = Q_{abs}I - 4\frac{H}{V_m}\frac{dr}{dt} \quad (1)$$

where ρ and C are the solid state mass density (kgm^{-3}) and heat capacity ($Jkg^{-1}K^{-1}$). The first term on the right hand side describes the laser heating, where I is the laser fluence (Wm^{-2}). Q_{abs} is the absorption efficiency, which can be determined from Mie theory. In the initial phase of particle heating the loss terms can be neglected. From the above an estimate for the heating time can be obtained. When a particle is heated up to a sufficiently high temperature, evaporation or decomposition become important. The flux of evaporated material from the particle surface is given by $n_s c/4$ where $c = (8k_bT/\pi M)^{1/2}$ and n_s is the density of the evaporated material at the cluster surface. Here M is the molecular mass of the released species (CF_2). The surface density n_s can be related to the surface temperature by the equilibrium Clausius-Clapeyron relation: $n_s k_b T = B\exp(-\theta/k_bT)$. Here θ and B are material dependent integration constants; θ reflects the energy needed to release a molecule from the surface (approximated by the H) and B the saturated vapor pressure. The values of the constants for the particle material are unknown and must be fitted to the experimental data. Finally the kinetic equation for the particle radius can be derived:

$$\frac{dr}{dt} = V_m\frac{c}{4}n_s = V_m\frac{c}{4}\frac{B}{k_bT}\exp(-H/k_bT) \quad (2)$$

In order to simulate the evaporation/decomposition process, Eqs. 1 and 2 will be integrated numerically.

Experimental

The teflon-like particles are formed in a capacitively coupled, parallel plate 13.56 MHz discharge, containing 10% CCl_2F_2 in argon. The pressure is 200 mTorr, the rf input power is 100 W and the total gas flow is 30 sccm. A detailed description

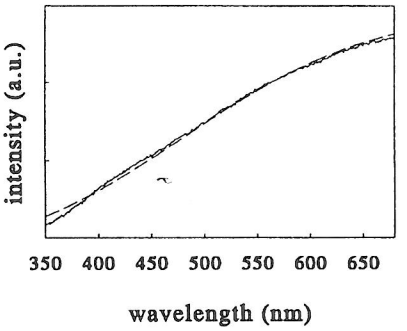

Figure 1: A typical emission spectrum (solid curve). The dashed curve is a blackbody fit to the data, corresponding to a temperature of 3600 K.

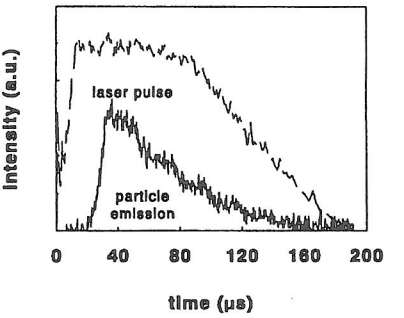

Figure 2: Wavelength integrated laser-induced emission ($\sim$ 300 - 1000 nm) from the particles under standard plasma conditions (solid curve) and normalized laser stray light (fluence: 8×10^8 Wm^{-2}, dashed curve).

of the setup is given elsewhere [4]. Some experiments have been performed in a 'dusty' argon plasma (i.e. a pure argon plasma, obtained by closing the CCl_2F_2 flow in an Ar/CCl_2F_2 plasma.

The measurements on particle heating have been performed using a Nd:YAG laser in the long pulse mode at 1064 nm. The pulse duration is 150 μs, the maximum available energy is about 0.5 J and the beam diameter is 2 mm. The time resolved emission spectra of the particles are recorded using the optical multichannel analyzer (OMA). The time resolved wavelength integrated emission intensity has been measured using a fast photo diode in combination with a digital oscilloscope. An optical filter (KG 3) has been used to discard scattering and stray light at 1064 nm. In the simulations of the emission intensities the appropriate transmission and sensitivity curves of the OMA, filter and photo diode have been incorporated.

Results and discussion

The radiation caused by the particle interaction with a strong infrared laser beam consists practically only of continuum, as can be seen in Fig. 1. No atomic or

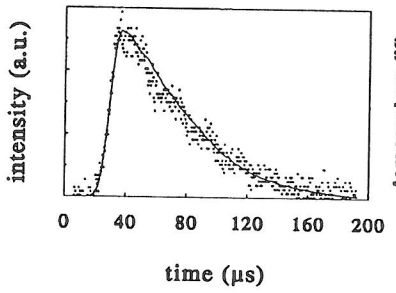

Figure 3: Wavelength integrated laser induced emission (dots, see Fig. 2), and the numerical fit (solid curve) for a 1 μm particle. The onset of the laser pulse is at t = 0 s.

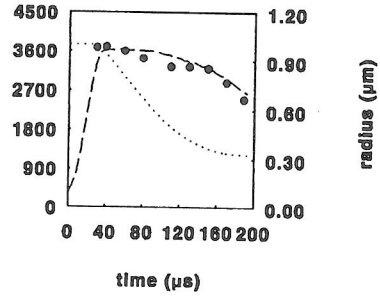

Figure 4: The calculated particle radius (dotted curve) and the measured (dots) and calculated (dashed curve) temperature during the decomposition process.

molecular line (band) emission has been found, even in the extinction phase. The wavelength dependence of the signal does change during the heating event. As the wavelength of the emitted light is smaller than the particle size, the shape of the continuum is best approximated by a simple Planck blackbody-like spectrum.

The wavelength integrated emission intensity as a function of time is shown in Fig. 2. Laser stray light, displaying the actual laser pulse shape, is collected on the window and given for comparison. The time delay between the laser onset and the emission onset corresponds to the heating time of the particle. In this period only little emission is observed, as the particle temperature is still low. The heating event has been simulated using Eqs. 1 and 2. The emission intensity is given by $r^2 P(\lambda, T)$, where P is Planck's function. The fit parameters are r, H and B. The particulate radius determines the heating time (the time delay of the maximum laser-induced emission signal) and the decomposition energy H is chosen so as to accommodate the experimentally determined particle temperature ($\sim$ 3600 K). Finally, r and B determine the decay of the emission, due to the decrease of the particle radius in time. In Fig. 3 the experimental and theoretical emission curves as a function of time are plotted. It can be seen that an excellent fit is obtained for $r = 1$ μm, $B = 4.2 \times 10^8$ Pa and $H = 3$ eV. The time dependence of the particle radius and temperature are shown in Fig. 4. It can be seen that also the measured time behavior of the temperature is well reproduced by the model. The temperature does not significantly change in time as long as

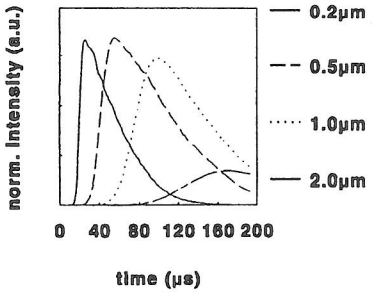

Figure 5: Calculated time dependent emission (normalized) for several particle sizes (r) for 2×10^8 Wm^{-2} laser fluence.

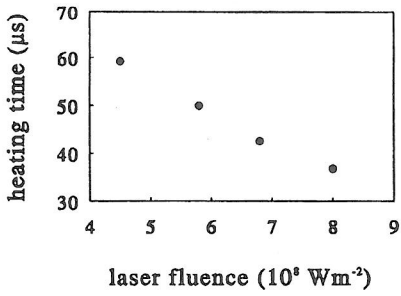

Figure 6: The heating time of particles as a function of laser fluence.

the decomposition takes place, as the energy losses due to decomposition balance the absorbed laser energy. As a result, $dT/dt \approx 0$ in Eq. 1.

The simulated emission curves for several particle sizes are shown in Fig. 5 (normalized to the particle surface, r^2). It can be seen that both the heating time and the decay time of the emission are functions of the particle radius. As the emission intensity is proportional to the particle density, this technique allows to determine both size and density from a single measurement. Eq. 1 predicts a variation of the heating time with the laser fluence, as shown in Fig. 6. The heating time has been determined by fitting the experimental data with the solutions of Eqs. 1 and 2. The total emission intensity and spectral temperature have been determined from the OMA spectra as a function of the laser fluence for three different plasma conditions (see Fig. 7). The emission intensities vary over several orders of magnitude, dependent on plasma conditions, but the temperatures are in all cases almost the same. This is an indication that the composition of particles does not depend on the dusty plasma conditions. The dashed curves in Fig. 7 are the dependences, predicted by the model. Again, a very good agreement with the experimental data is obtained. The temperature increases strongly with laser fluence until the temperature is reached, at which decomposition becomes important (about 3000 K at 10^8 Wm^{-2}). For fluences higher than this 'threshold' value only a weak temperature increase is found. The decomposition speed increases linearly with the laser power, which implies that at high fluences the particles are destroyed faster and consequently the duration of the whole event is shorter.

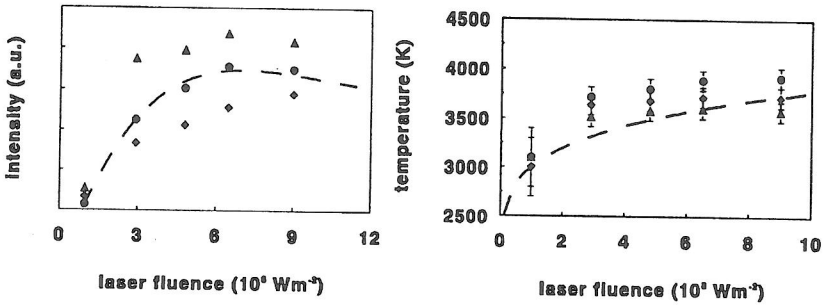

Figure 7: The laser-induced emission intensity (left) and the spectral temperature (right), obtained from the OMA spectra as a function of the laser fluence (200 mTorr, 100 W and 30 sccm). Circles: 5% CCl_2F_2, 1 cm above the rf electrode (Intensity $\times 5$), triangles: 'dusty' Ar plasma, 1 cm above the rf electrode ($r \approx 1$ μm), diamonds: 'dusty' Ar plasma, 2.5 cm above the rf electrode ($r \leq 100$ nm), (Intensity $\times$ 100). The dashed curves represent simulations for a 1 μm particle.

Therefore it can be understood that the time integrated emission at high fluences saturates and eventually decreases.

This project is funded by the European Community under the BRITE/EURAM programme contract no. BRE2-CT94-0944.

References

[1] Nato Advanced Workshop on the Formation, Transport and Consequences of Particles in Plasmas, Chateau de Bonas, Castura-Verduzan, France Aug./Sept. 1993 . *Plasma Sources Sci. Technol.* **3**. vol. 3, 1994.

[2] Special issue on charged dust in plasmas. *IEEE Trans on Plasma Sci.* **22**. vol. 2, 1994.

[3] E. Stoffels, W.W. Stoffels, D. Vender, G.M.W. Kroesen, and F.J. De Hoog. *IEEE Trans. Plasma Sci.***22**. 116, 1994.

[4] E. Stoffels and W.W. Stoffels. *Electrons, ions and dust in a radio-frequency discharge.* Ph.D Thesis, Eindhoven University of Technology, 1994.